

Semihard scattering unraveled from collective dynamics at $\sqrt{s} = 17$ GeV

Jana Bielcikova[†] for the CERES/NA45 Collaboration

Physics Department, Yale University, P.O. Box 208120, New Haven, CT 06520-8120, USA

Abstract. We present a study of elliptic flow (v_2) and two-particle azimuthal correlations of charged hadrons and high transverse momentum (p_T) pions measured by the CERES experiment in Pb+Au collisions at $\sqrt{s} = 17$ GeV. Azimuthal anisotropy v_2 increases linearly with p_T to a value of 10% at $p_T = 1.5$ GeV/ c . Beyond this p_T the slope decreases indicating a possible saturation at high p_T . Two-pion azimuthal anisotropies ($p_T > 1.2$ GeV/ c) exceed v_2 by about 60% in semicentral collisions and reveal non-harmonic contributions at close ($\Delta\phi \approx 0$) and back-to-back ($\Delta\phi \approx \pi$) angles that can be attributed to semihard processes. While the close-angle peak remains unchanged, the back-to-back peak is broadened and disappears in central collisions.

1. Introduction

Elliptic flow is an important signature of collective dynamics in non-central heavy-ion collisions at high energies. It is driven by anisotropic pressure gradients built up during the early stage of the collision due to the geometrically anisotropic overlap zone of the colliding nuclei. Moreover, it carries information on such important issues as the equation of state (EOS) and the level of equilibration achieved. Elliptic flow manifests itself in an azimuthal anisotropy of particle yields with respect to the reaction plane. Two-particle azimuthal correlations are sensitive to elliptic flow but at large transverse momenta (p_T) are expected to reveal also relics of semihard scattering. We report about successful attempts to trace primeval partonic scattering at $\sqrt{s} = 17$ GeV by two-particle azimuthal correlations of pions at moderately large p_T ($p_T > 1.2$ GeV/ c).

2. Experimental setup and particle tracking

Figure 1 shows the CERES experimental setup from 1996. The spectrometer covers a pseudo-rapidity range $2.1 < \eta < 2.65$ and has full azimuthal acceptance, which is important for studies of azimuthal distributions. Although the overall design was optimized to detect low-mass dilepton pairs [3], CERES offers many capabilities in hadronic physics as well. Charged particle tracks are reconstructed on a statistical basis combining information from two radial silicon drift detectors (SDD1, SDD2) placed closely behind the target and a multi-wire proportional chamber (PADC) behind a magnetic field used for momentum determination. Charged pions are identified and distinguished from electrons by smaller ring radii in two ring-imaging

[†] jana.bielcikova@yale.edu

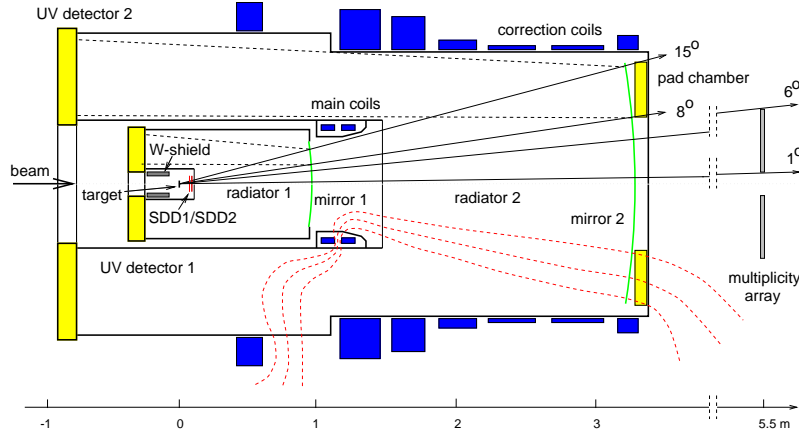


Figure 1. CERES experimental setup in 1996.

Cherenkov detectors (RICH1, RICH2). Since the RICH detectors are filled with CH_4 with a high Cherenkov threshold ($\gamma_{th} \simeq 32$), only pions with $p > 4.5 \text{ GeV}/c$ produce Cherenkov light. Figure 2 shows the correlation between the ring radius in RICH2 and the azimuthal deflection in magnetic field with the two islands corresponding to negatively and positively charged pions, respectively. Pion momenta are determined from the ring radius measurement due to its higher precision in comparison to the deflection in magnetic field [2].

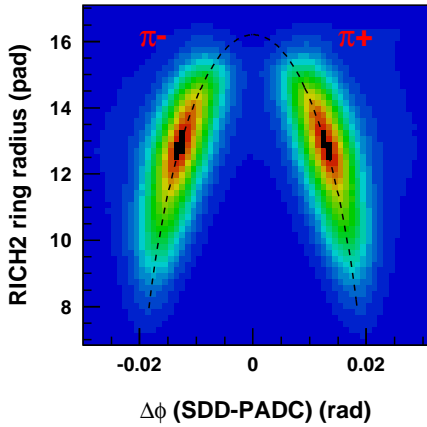


Figure 2. Correlation between the pion ring radius in RICH2 and the azimuthal deflection in the magnetic field measured between SDDs and PADC. The dashed line represents the expected correlation.

3. Centrality determination

We have analyzed $41 \cdot 10^6$ Pb+Au collisions taken at $\sqrt{s} = 17 \text{ GeV}$. The centrality was determined offline using the number of charged particles N_{ch} measured by the SDD in $2 < \eta < 3$. The N_{ch} distribution corrected for efficiency losses is shown in Fig. 3. As the multiplicity detector used as a centrality trigger suffered from voltage instabilities, which were unfortunately not continuously monitored, we had to use the

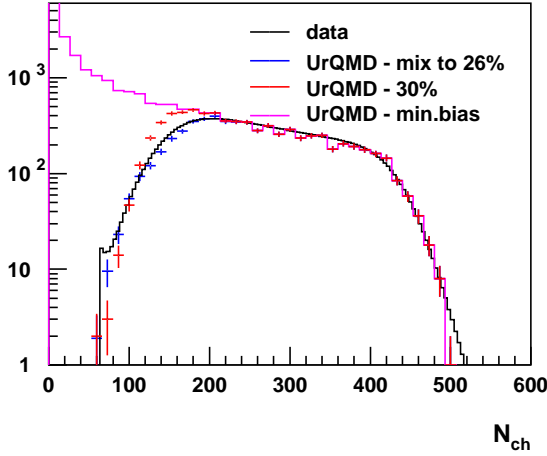


Figure 3. Charged particle multiplicity N_{ch} measured by the silicon drift detectors in the pseudorapidity interval $2 < \eta < 3$. The data are corrected for efficiency losses and compared to UrQMD calculations for various centrality selections as given in the legend. An overall multiplicative factor of 1.03 was applied to N_{ch} values from UrQMD in order to describe the data in central collisions.

UrQMD model [4] to estimate the fraction of geometrical cross section σ_{geo} measured. We have concluded that the measured data sample corresponds to the most central ($26.0 \pm 1.5\%$) of σ_{geo} . The data sample was divided into 6 centrality classes summarized in Table 1 together with the corresponding fraction of geometrical cross section σ/σ_{geo} , impact parameter b , number of participants N_{part} , and binary collisions N_{coll} obtained from a Glauber calculation neglecting fluctuations [5].

Class	Events (10^6)	N_{ch}	$\sigma/\sigma_{geo}(\%)$	b (fm)	N_{part}	N_{coll}
1	7.77	147	21 - 26	6.8 - 7.5	159	293
2	6.58	198	17 - 21	6.0 - 6.8	189	368
3	5.66	234	13 - 17	5.3 - 6.0	222	453
4	6.06	273	9 - 13	4.4 - 5.3	255	542
5	6.05	321	5 - 9	3.4 - 4.4	289	639
6	8.16	395	< 5	< 3.4	336	774

Table 1. Definition of centrality classes.

4. Collective elliptic flow

The strength of elliptic flow is commonly quantified by the second Fourier coefficient v_2 [6] of azimuthal particle distributions with respect to the reaction plane Ψ_R

$$\frac{dN}{d(\phi - \Psi_R)} = A \left(1 + \sum_{n=1}^{\infty} 2 v_n \cos(n(\phi - \Psi_R)) \right). \quad (1)$$

A priori, the reaction plane is unknown and is therefore estimated on an event-by-event basis from charged particle tracks measured by the SDDs using a subevent method. Non-uniformities in the event plane distribution are removed by standard procedures [6]. Depending on centrality of a given collision, the r.m.s. of the event plane resolution is 35-40 degrees.

The centrality and p_T dependence of v_2 corrected for the event plane dispersion is shown in Fig. 4. In addition, the $v_2(p_T)$ data points are corrected for Bose-Einstein

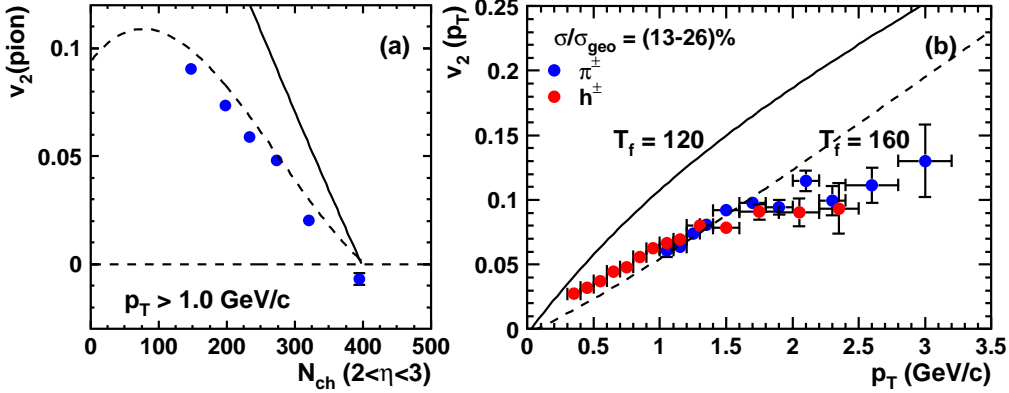


Figure 4. Centrality (a) and p_T dependence (b) of v_2 for charged pions and hadrons as indicated in the legend. Hydrodynamical calculations [10] with a phase transition at $T_c = 165$ MeV are shown for kinetic freeze-out temperature $T_f = 120$ MeV (solid line) and $T_f = 160$ MeV (dashed line). The quoted errors are statistical only. The absolute systematic errors vary between 0.5% and 1.5% going from semicentral to central collisions.

correlations [2, 7, 8]. Since this correction procedure becomes questionable for central collisions, the centrality dependence of v_2 was left uncorrected. We observe that v_2 decreases approximately linearly with centrality and vanishes in the most central collisions with no remaining asymmetry in the overlap zone present (Fig. 4a). The p_T dependence of v_2 in semicentral collisions (Fig. 4b) shows a linear rise below $p_T = 1.5$ GeV/c. Beyond $p_T \approx 1.5$ GeV/c the slope decreases, possibly indicating a saturation of v_2 at high p_T similar to observations at RHIC [9].

A direct quantitative comparison with a hydrodynamical calculation [10] using an EOS with a first order transition to a quark gluon plasma at temperature $T_c = 165$ MeV favors a higher freeze-out temperature $T_f = 160$ MeV rather than a lower one, $T_f = 120$ MeV. However, $T_f = 120$ MeV is necessary in order to describe the p_T spectra of protons. Possible explanations might be either incomplete thermalization or a necessity to include viscous effects into calculations [11].

5. Azimuthal correlations at high- p_T

We turn to the measurement of two-particle azimuthal correlations of high- p_T pions. The two-particle distributions in semicentral collisions corrected for single-track reconstruction efficiency are shown in Fig. 5. At small opening angles, overlapping rings in the RICH detectors cause a dip around $\Delta\phi \approx 0$ (Fig. 5a). This instrumental effect can be cured by using either a Monte-Carlo (MC) correction or by enforcing a full ring separation by imposing a cut in polar angle difference $\Delta\theta$. We have made a compromise between the two methods and use the separation cut $\Delta\theta > 20$ mrad (Fig. 5b) which still keeps about 60% of pion data sample while reducing sensitivity to the MC correction by a factor of four. The corrected distributions reveal a strong anisotropy with maxima at close ($\Delta\phi \approx 0$) and back-to-back ($\Delta\phi \approx \pi$) angles.

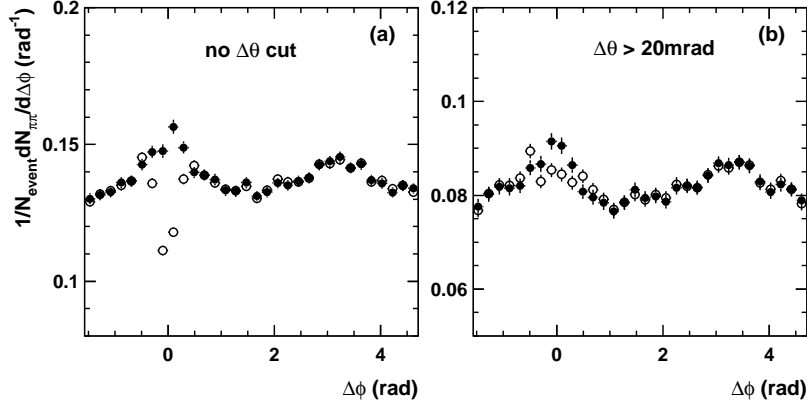


Figure 5. Two-pion azimuthal distributions ($p_T > 1.2$ GeV/ c) for the centrality class C1 (a) without and (b) with a $\Delta\theta > 20$ mrad cut applied. Open symbols: data only after the MC correction for single track reconstruction efficiency. Closed symbols: data after an additional MC correction of the finite two-track resolution.

The two-particle distributions can be decomposed again using a Fourier method

$$\frac{dN}{d\Delta\phi} = B \left(1 + \sum_{n=1}^{\infty} 2 p_n \cos(n\Delta\phi) \right), \quad (2)$$

where $\Delta\phi$ is an azimuthal angle difference between any two pions in a given event. If only correlations due to collective flow are present, then $p_n = v_n^2$. Figure 6 shows a comparison of the $\sqrt{p_2}$ values with v_2 obtained from the event plane method. We observe that the $\sqrt{p_2}$ values are systematically larger than v_2 . A closer look at the

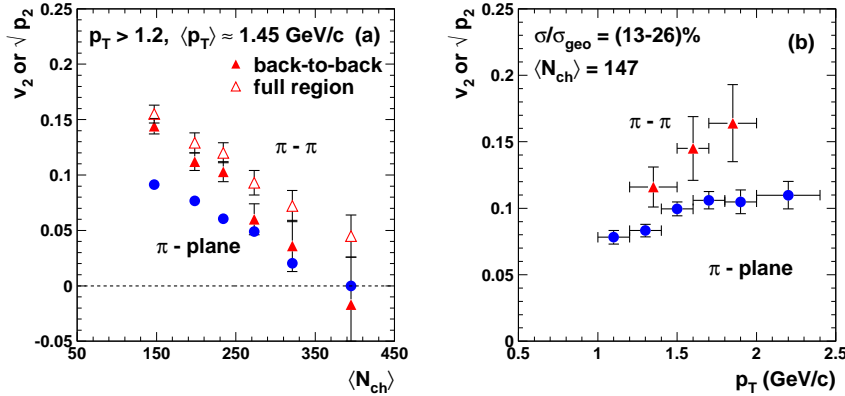


Figure 6. Comparison of v_2 (circles) obtained from the event plane method and $\sqrt{p_2}$ (triangles) from two-pion azimuthal correlations. (a) Centrality dependence for full azimuth (open triangles) and a range restricted to the back-to-back peak ($|\Delta\phi| \geq 0.6$ rad, closed triangles). (b) p_T dependence for the centrality class C1.

centrality dependence shows that the anisotropy in the back-to-back region approaches zero for central collisions while the close-angle correlations persist even in the most central collisions. The gap between v_2 and $\sqrt{p_2}$ seems to increase with increasing p_T (Fig. 6b). Unfortunately, the statistical significance of this measurement is degraded by invoking a two-dimensional window in p_T .

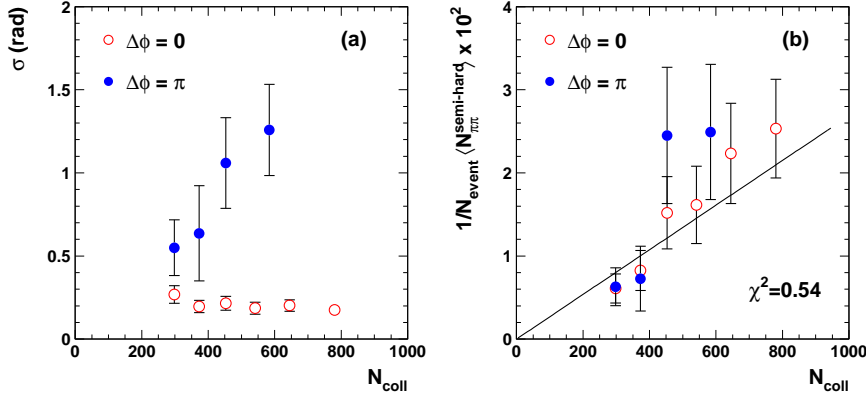


Figure 7. Centrality dependence of (a) the Gaussian widths and (b) the yield of close-angle (open symbols) and back-to-back (full symbols) correlation peaks for pions with $p_T > 1.2$ GeV/ c .

Assuming the observed excess is due to correlations of semihard origin, we have fit the distributions with two Gaussian peaks at $\Delta\phi = 0$ and π on top of the elliptic flow modulated background. The fit parameters are the Gaussian amplitudes, widths and background, while v_2 is fixed from the event plane method. The close-angle peak remains narrow (Fig. 7a) at $\sigma_0 = (0.23 \pm 0.03)$ rad averaged over the measured centrality. The corresponding average momentum perpendicular to the partonic transverse momentum [12] is $\langle |j_{Ty}| \rangle = (190 \pm 25)$ MeV/ c which is similar although somewhat lower than ISR [13] and RHIC [12] measurements. The back-to-back peak broadens with centrality and escapes detection in central collisions. The last measured point ($N_{coll} = 600$) corresponds to $\langle |k_{Ty}| \rangle = (2.8 \pm 0.6)$ GeV/ c which agrees well with preliminary results from central Au+Au collisions at RHIC [12]. Within the statistical errors, the yield of the close-angle and back-to-back pion pairs, defined as an area under the Gaussian peak (Fig. 7b), grows linearly with N_{coll} which supports the suggested interpretation of semihard scattering.

Due to asymmetry of the overlap zone in non-central collisions, the pion yield might be suppressed if pions propagate perpendicular to the reaction plane rather than along it. We have constructed azimuthal distributions confining one of the pions in the region of $\pm\pi/4$ around the reconstructed event plane (*in-plane*) or perpendicular to it (*out-of-plane*). The distributions corrected for efficiency losses are shown in Fig. 8. For both in-plane and out-of-plane regions, the data lie above the expectations from elliptic flow [14]. After subtracting the flow contributions, we have extracted the ratios of yields in-plane with respect to those out-of-plane. For the close-angle peak this ratio is 1.32 ± 0.37 and 1.39 ± 0.44 for the back-to-back component. An additional systematic error of 15% was estimated due to uncertainties in the subtraction of the elliptic flow

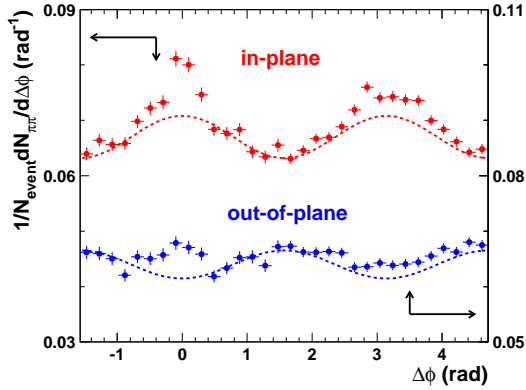


Figure 8. In-plane (top) and out-of-plane (bottom) two-pion azimuthal correlations for $p_T > 1.2 \text{ GeV}/c$ and $\Delta\theta > 20 \text{ mrad}$. Dashed lines are the expectations for pure elliptic flow v_2 measured by the event plane method. Data are averaged over centrality classes C1, C2, and C3.

contribution. Within the given errors, we can conclude that both components bear only a weak, if any, preference to the reaction plane orientation.

6. Conclusion

In summary, we have discussed properties of semihard azimuthal correlations of high- p_T pions embedded in collective flow at SPS energy. The observed non-flow components, presumably of semihard origin, show similar but also important differences to observations at RHIC [15, 16]. The close-angle peak remains narrow at all measured centralities, consistent with fragmentation, while the back-to-back component broadens and disappears in background in the most central collisions. In addition, there seems to be only a weak, if any, preference of semihard pion pairs to the orientation of the reaction plane. This is different from recent findings at RHIC [16] showing a stronger suppression of high- p_T correlations out of the reaction plane.

References

- [1] Agakichiev G *et al.* (CERES) 2004 *Phys. Rev. Lett.* **92** 032301
- [2] Slivova J 2003 PhD thesis, Charles University, Prague
- [3] Lenkeit B *et al.* (CERES) 1999 *Nucl. Phys.* **A661** 23
- [4] Bass SA *et al.* 1998 *Prog. Part. Nucl. Phys.* **41** 225
- [5] Eskola KJ, Kajantie K and Lindfors J 1989 *Nucl. Phys.* **B323** 37; Miskowiec D, <http://www.gsi.de/~misko/overlap>
- [6] Poskanzer AM, Voloshin SA 1998 *Phys. Rev.* **C68** 1671
- [7] Dinh PM, Borghini N and Ollitrault J-Y 2000 *Phys. Lett.* **B477** 51; private communication
- [8] Adamova D *et al.* (CERES) 2003 *Nucl. Phys.* **A714** 124
- [9] Ackermann KH *et al.* (STAR) 2001 *Phys. Rev. Lett.* **86** 402; Adcox K *et al.* (PHENIX) 2002 *Phys. Rev. Lett.* **89** 212301
- [10] Kolb PF, Huovinen P, Heinz UW, Heiselberg H 2001 *Phys. Lett.* **B500** 232; Huovinen P, private communication
- [11] Teaney D nucl-th/0204023; nucl-th/0301099
- [12] Rak J *et al.* (PHENIX) 2004 *J. Phys.* **G30** S1309-S1312
- [13] Angelis ALS *et al.* (CCOR) 1980 *Phys. Lett.* **B97** 163
- [14] Bielcikova J, Esumi S, Filimonov K, Voloshin S and Wurm JP 2004 *Phys. Rev.* **C69** 021901
- [15] Adler C *et al.* (STAR) 2003 *Phys. Rev. Lett.* **90** 082302
- [16] Adams J *et al.* (STAR) nucl-ex/0407007